JOURNAL OF VIROLOGY, Sept. 1990, p. 4108–4114
0022-538X/90/094108-07$02.00/0

Vol. 64, No. 9

Bovine Coronavirus mRNA Replication Continues throughout Persistent Infection in Cell Culture

MARTIN A. HOFMANN, PHIROZE B. SETHNA, AND DAVID A. BRIAN*

Department of Microbiology, University of Tennessee, Knoxville, Tennessee 37996-0845

Received 2 March 1990/Accepted 26 May 1990

The existence of viral mRNA replicons was demonstrated in cells infected with the bovine coronavirus by showing a minus-strand counterpart and a corresponding replicative intermediate for each subgenomic mRNA species. mRNA replication is thus a universal property of coronaviruses, since this is now the third coronavirus for which it has been demonstrated. During the acute phase of infection (first 48 h), minus and plus strands accumulated at the same rate initially, but maximal accumulation of minus strands peaked earlier than that for plus strands, indicating that minus- and plus-strand levels are differentially regulated. In addition, packaged (input) mRNAs appeared to serve as templates for their own early replication. mRNA replication continued throughout establishment and maintenance of persistent infection (studied for 120 days), which is consistent with our hypothesis that mRNA replication contributes mechanistically to virus persistence. A replication-defective (potentially interfering) species of RNA existed transiently (beginning at day 2 and ending before day 76 postinfection), but because of its transient nature it cannot be considered essential to the long-term maintenance of virus persistence.

We have recently shown that during replication of the porcine transmissible gastroenteritis coronavirus (TGEV), a minus-strand copy of each polyadenylated, subgenomic mRNA molecule is made (22). We demonstrated that (i) the rate of synthesis of subgenomic minus strands (number of molecules per unit time) exceeded that for the antigenome, (ii) the time of peak minus-strand accumulation occurred earlier than that for peak plus-strand accumulation, and (iii) subgenomic replicative intermediates exist. We therefore demonstrated the existence of mRNA replicons and postulated two biological consequences of this phenomenon: (i) mRNA replication is an important mechanism by which coronaviruses amplify mRNAs, and (ii) replicating mRNAs play a role in the establishment of persistent infections, since they could, in theory, function as genomes of defective interfering viruses to attenuate replication of full-length genome.

To establish whether mRNA replication is a general property of coronaviruses and, if so, to test our hypothesis that mRNA replicons play a role in the establishment of persistent infection, we have studied the synthesis of bovine coronavirus (BCV) RNAs in cell culture throughout acute infection and during establishment of a persistent infection. BCV was chosen because it is evolutionarily diverged from TGEV and because it readily establishes persistent infection with a high cell survival rate (estimated to be greater than 80%) throughout the acute infection.

In this study, we demonstrate for a second coronavirus that subgenomic mRNAs undergo replication through a minus-strand copy of each mRNA and that mRNA replication continues throughout the development and maintenance of persistent infection in a cell culture for at least 120 days. The results are consistent with our hypothesis that coronavirus mRNA replicons contribute to the establishment and maintenance of persistent infection. The appearance of a defective plus-strand RNA species and its minus-strand counterpart is also reported, but its existence was transient (beginning at day 2 and ending before day 76 postinfection), and although it may have contributed in part to the establishment of the persistent infection, it cannot be considered essential to the long-term maintenance of virus persistence.

* Corresponding author.

MATERIALS AND METHODS

Preparation of RNA from uninfected and acutely infected cells and from cells throughout establishment and maintenance of persistent infection. The Mebus strain of BCV was plaque-purified three times and grown on a human rectal tumor (HRT) cell line as described previously (10, 14). Stock virus inoculum (infectious titer of 3×10^7 PFU/ml) was prepared by passaging virus three times at a multiplicity of ≈1 and clarifying the culture supernatant by centrifugation at 2,500 × *g* for 10 min.

For preparation of RNA at times throughout acute infection (0 to 48 h postinfection [hpi]), cells in dishes at 80% confluency were infected at a multiplicity of ≈3, incubated for 1 h at 37°C, and rinsed twice with Earle balanced salt solution containing 20 mM HEPES (*N*-2-hydroxyethylpiperazine-*N'*-2-ethanesulfonic acid), and RNA was either extracted immediately (0 hpi) or cells were refed with growth medium and RNA was extracted at 1, 2, 3, 4, 5, 6, 8, 10, 12, 15, 18, 21, 24, 36, and 48 hpi. Cytoplasmic RNA from infected and uninfected cells was extracted by the Nonidet P-40 lysis-proteinase K digestion method and quantitated as described previously (22).

For preparation of RNA at times throughout establishment and maintenance of persistent infection (2 to 120 days), cells in flasks and plates were infected as described above and incubated at 37°C for 4 days. Cells in plates were used for RNA harvesting, while those in flasks were passaged at a ratio of 1:4 to prepare two flasks for maintaining infected cells and two plates for RNA harvesting 4 days later. Cells were subsequently passaged, and RNA was extracted every 4 days (days 8 through 40 postinfection [p.i.]) or at 76 and 120 days p.i.

Preparation of virion RNA. BCV from cell culture supernatant harvested at 48 hpi was purified by isopycnic sedimentation in sucrose gradients, and RNA was extracted by the sodium dodecyl sulfate (SDS)-proteinase K method (14).

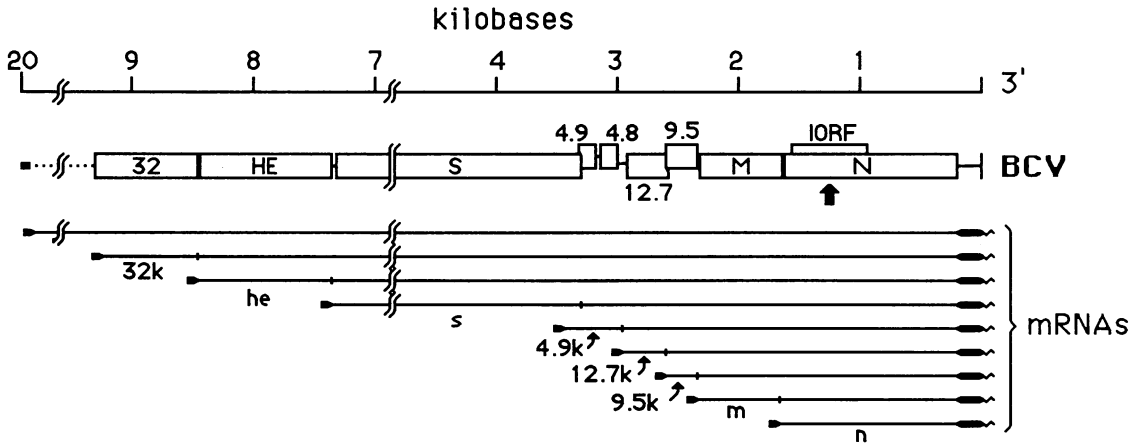

FIG. 1. Structural relationships among the BCV genome, mRNAs, and synthetic oligodeoxynucleotide probes. The nine open reading frames deduced from primary sequence of the 3' end of the BCV genome are drawn to scale. They are identified as HE for hemagglutinin-esterase protein, S for spike protein, M for membrane protein, N for nucleocapsid protein, and by size (in kilodaltons) for potential nonstructural proteins. Their corresponding mRNAs are identified as he, s, m, n, 32k, 4.9k (this transcript contains both the 4.9- and 4.8-kDa open reading frames), 12.7k, and 9.5k. There is no mRNA identified for the internal open reading frame (IORF) within the *N* gene. The site from which the oligodeoxynucleotide probes were derived is indicated by a large arrow. The 5' leader sequence (80 bases) and the 3' noncoding sequence (291 bases) are indicated by heavy lines and are drawn to scale. The 3' poly(A) tail is indicated by a wavy line. The largest mRNA, which serves as a template for synthesis of viral polymerase, is presumably identical to the genome.

Northern (RNA blot) analyses. For preparation of probes, the 26-base sequence 5'-TGGGAATCTTGACGAGCCCCA GAAGG-3' from within the N gene (14), having a G+C content of 65%, was chosen, and a synthetic oligodeoxynucleotide complementary to this sequence was made and designated probe 1. Probe 2 was prepared as an oligodeoxynucleotide having the virus sense of this sequence. Probes 1 and 2 therefore hybridized to plus- and minus-strand RNAs, respectively. Oligodeoxynucleotides were purified by preparative gel electrophoresis in 20% nondenaturing polyacrylamide gels, and the concentration of the final product was determined by A_{260}, with 1 A_{260} unit being equivalent to 20 μg/ml. Then, 250 ng (27.5 pmol) of oligodeoxynucleotide was endlabeled with [γ-^{32}P]ATP by the forward reaction and purified by size exclusion chromatography as described before (22) except that Bio-Spin 30 (Bio-Rad Laboratories) columns were used. For determining the specific activity of the labeled product, it was assumed that all of the oligodeoxynucleotide had been recovered, and radioactivity was quantitated with the Ambis Radioanalytic Imaging System (Ambis, San Diego, Calif.) after measured samples were spotted onto Nytran membranes (Schleicher & Schuell).

Electrophoretic separation of RNA and blotting onto Nytran membrane were done as described previously (22) except that 12 μg of cytoplasmic RNA or 5 ng of virion RNA was loaded per lane. RNase-resistant species in double-stranded replicative forms were analyzed as described previously (22). Essentially, cytoplasmic RNA harvested at various times p.i. was digested with 10 μg of RNase A per ml in the presence of 300 mM NaCl, and RNase-resistant species were identified by Northern analyses. Quantitation was accomplished by scanning with the Ambis system. The average number of molecules of each RNA species per cell was calculated from the specific activity of the respective probe and from our measured yield of 12 μg of RNA per 7.2 × 10^5 cells. All quantitation assumed that cells were confluent, and no correction was made for subconfluency at 0 hpi and early times after infection.

Immunofluorescence. Cells were grown on LabTek chamber slides (Nunc, Naperville, Ill.) and examined for cytoplasmic fluorescence with rabbit antiserum prepared against gradient-purified, SDS-disrupted BCV. Cells were fixed at 24 hpi in the case of acute infection or at 48 h after passaging in the case of persistent infection with ice-cold absolute ethanol for 15 min at −20°C. Fixed cells were incubated for 1 h at 37°C with a 1:40 dilution of antiserum or nonimmune rabbit serum and subsequently with a 1:50 dilution of goat anti-rabbit immunoglobulin G-fluorescein isothiocyanate conjugate (Boehringer Mannheim Biochemicals, Indianapolis, Ind.) for 1 h at 37°C.

RESULTS

BCV mRNAs undergo replication, and packaged mRNA from input virus may serve as template for early replication. We and others have shown that BCV synthesizes nine mRNA species, numbered 1, 2, 2-1, 3, 4, 5, 5-1, 6, and 7 in recently recommended terminology (4, 8). Based on sequence data and Northern analyses, they are predicted to encode, respectively, the RNA-dependent RNA polymerase (mRNA 1), a 32-kilodalton (kDa), possibly nonstructural protein (mRNA 2) (5), the hemagglutinin-esterase glycoprotein (HE) (mRNA 2-1) (9, 18), the large spike structural glycoprotein (S) (mRNA 3) (1), 4.9- and 4.8-kDa nonstructural proteins on one transcript (mRNA 4) (S. Abraham, T. E. Kienzle, W. E. Lapps, and D. A. Brian, Virology, in press), a 12.7-kDa nonstructural protein (mRNA 5) (Abraham et al., in press), a 9.5-kDa nonstructural protein (mRNA 5-1) (Abraham et al., in press), the integral membrane structural glycoprotein (M) (mRNA 6) (14), and the nucleocapsid structural glycoprotein (N) (mRNA 7) (14) (Fig. 1).

To confirm that these could each be identified by hybridization to probe 1 and to establish the kinetics of their synthesis, a Northern analysis was done with cytoplasmic RNA collected at various times after infection (Fig. 2A and C). Because of the 3' nested-set structure of BCV mRNAs, probe 1, representing a sequence from within the N gene, should hybridize to n and all larger mRNA species. As controls, RNAs from purified virus and from uninfected cells

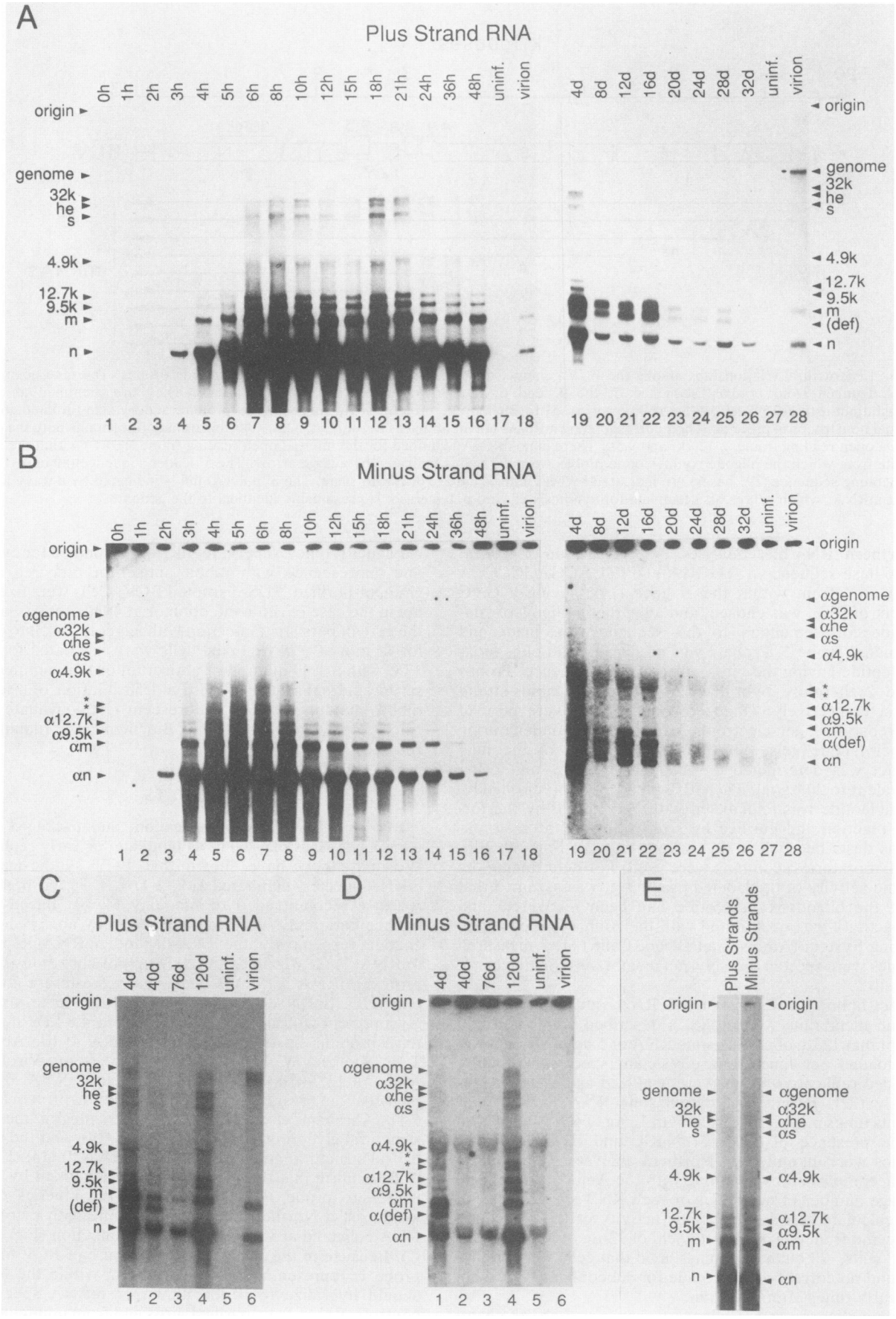
A
Plus Strand RNA
origin
0h 1h 2h 3h 4h 5h 6h 8h 10h 12h 15h 18h 21h 24h 36h 48h uninf. virion
4d 8d 12d 16d 20d 24d 28d 32d uninf. virion
origin
genome
32k
he
s
4.9k
12.7k
9.5k
m
n
(def)
1 2 3 4 5 6 7 8 9 10 11 12 13 14 15 16 17 18
19 20 21 22 23 24 25 26 27 28
B
Minus Strand RNA
αgenome
α32k
αhe
αs
α4.9k
α12.7k
α9.5k
αm
αn
α(def)
C
Plus Strand RNA
4d 40d 76d 120d uninf. virion
1 2 3 4 5 6
D
Minus Strand RNA
E
Plus Strands
Minus Strands

were included. The following points emerged from this analysis. (i) No RNA from uninfected cells was detectable, establishing the viral specificity of probe 1. (ii) Virus purified by isopycnic sedimentation on sucrose gradients contained, in addition to genome, all eight subgenomic mRNA species. Strikingly, n and m were present in greater molar abundance than genome. In this electrophoresis and transfer system, approximately 60% of genome-size RNA and 80% of N mRNA-size RNA are transferred (unpublished data). Even after correcting for this difference, more molecules of n and m were packaged than genome. The mRNA molecules apparently do not represent species adventitiously bound to the virion surface, since digestion with RNase A prior to virus purification made no difference in the profile of extracted RNA (unpublished data). (iii) From immediately after infection (0 hpi) through 2 hpi, 2 to 15 and 0 to 2 molecules, respectively, of n and m were detected per cell (Fig. 3A). No other species, including genome, were found at these times. We do not know to what extent these may represent RNA molecules from bound but noninternalized virions. (iv) An increase in mRNA numbers was first detected by 3 hpi, and these were for n and m (Fig. 3A). An increase in the number of all mRNAs was observed by 4 hpi. The dramatic early and rapid increase in the number of n and m mRNAs suggests that input mRNAs are serving as templates for replication. mRNA numbers for all species reached a maximum at 8 hpi and remained near maximal levels through 20 hpi (Fig. 3A). (v) A new species, an apparently defective RNA intermediate between n and m in size (identified as species def in Fig. 2A and C) appeared by 48 hpi and persisted for at least 40 days (discussed below).

To determine whether subgenomic minus-strand counterparts to BCV mRNAs exist, Northern blots from an identical electrophoretic preparation were analyzed with probe 2. A minus-strand counterpart for each mRNA was found, including one for the newly identified def species (Fig. 2B and D). In addition, two minus-strand species that apparently had no plus-strand counterpart were observed (identified by asterisks in Fig. 2B and D). Although probe 2 could be endlabeled to the same specific activity as probe 1, a longer exposure was required to obtain an autoradiogram of similar density, suggesting that minus strands were fewer in number. No RNA from uninfected cells was identified with probe 2 except for small amounts of 28S and 18S rRNAs. This quantity was subtracted during quantitation of comigrating viral species.

We conclude that probe 2 is specifically detecting minus-strand RNA species and not merely abundant mRNA molecules for the following reasons. (i) Probe 2 did not detect virion genomic RNA or any of the packaged mRNA species. (ii) The time of maximal minus-strand accumulation was strikingly different from that for plus-strand (Fig. 3A and B, and Discussion below). (iii) Minus-strand species migrated distinctly faster than their corresponding mRNAs. This was especially apparent when RNAs were analyzed in adjacent lanes (Fig. 2E).

Especially noteworthy is the early appearance of the minus-strand species and the rapid accumulation of both αn and αm. We had noted earlier for TGEV (22) that the rate of both plus- and minus-strand synthesis, in terms of number of molecules accumulated per unit time, was inversely related to molecular length. The same holds true for BCV (note the steeper slopes for the shorter molecules in Fig. 3A and B), but in addition, n got a strikingly earlier start at replication, suggesting that its presence as input template may be playing a role in its early synthesis. There may be, therefore, two factors contributing to the rapid accumulation of the shorter mRNAs over genome: (i) shorter length and (ii) greater abundance in input virus particles.

Initial synthesis of minus and plus strands appears to be simultaneous, but their levels are differentially regulated late in acute infection. From the data shown in Fig. 2A and B and 3A and B, we make the following observations. (i) The initial synthesis of minus and plus strands occurred simultaneously and at similar rates, as determined by measuring the rates of RNA accumulation. It can be noted, for example, that between 2 and 3 hpi, n increased from 15 to 120 molecules per cell, whereas αn increased from approximately 10 to 100 (Fig. 3A). For the same period, m increased from 2 to 30 and αm increased from 0 to 15 molecules per cell. (ii) The time of maximal minus-strand accumulation occurred earlier (at 6 hpi) than that for plus-strand (at 8 hpi), and minus-strand numbers began to diminish earlier and with a steeper slope than plus-strand numbers.

The notion that minus and plus strands are initially synthesized concurrently was supported by a second set of experiments in which RNase-resistant RNA species in replicative forms were sought. Whereas with TGEV we found primarily RNase-resistant minus strands during times of peak plus-strand synthesis (22) (i.e., representing a structure in which the species serving as template for multiple progeny molecules would be fully protected, and the nascent chains [tails] would be shortened dramatically), for BCV we found equal numbers of protected minus and plus strands from 2 to 12 hpi (data not shown). Such a structure would be expected if templates for synthesis of minus and plus strands were present in equal numbers (and hence generating products at an equal rate).

Since hybridization analyses quantitate only the total number of accumulated molecules, the relative importance of continuing RNA synthesis and RNA degradation in giving rise to the different population decay rates after 8 hpi (Fig. 3B) cannot be measured by this method. Further experimentation is required to differentiate between these two possibilities.

mRNA replication continues throughout establishment and maintenance of persistent infection. As a first step in testing our hypothesis that replicating mRNAs play a role in establishing and maintaining persistent infection, we sought evidence for continued mRNA replication throughout the first 120 days p.i. Figures 2C and D and 3C and D illustrate that whereas numbers of both plus and minus strands continued

FIG. 2. Identification of plus- and minus-strand RNA species in BCV-infected cells. RNA from purified virions or from the cytoplasm of uninfected (uninf.) or infected cells was electrophoresed, blotted, and hybridized with probe 1 (A and C) or probe 2 (B and D). Times postinfection are shown above the lanes (d, days). α indicates antisense or minus-strand polarity; (def) identifies a defective RNA species; and asterisks identify uncharacterized RNA species (see text). RNA used in panel E was obtained at 6 hpi and electrophoresed in adjacent lanes but probed separately after transfer to Nytran membrane. (A) Lanes 1 through 18 were exposed to Kodak X-Omat film for 6 h without an intensifying screen, and lanes 19 through 28 were exposed for 16 h without a screen. (B) Lanes 1 through 18 were exposed for 4 days with a screen, and lanes 19 through 28 were exposed for 7 days with a screen. Panel C was exposed for 5 h without a screen, and panel D was exposed for 10 days with a screen. All exposures were made at −80°C. (Radioactivity at the origin is known to be probe nonspecifically bound to a pencil mark on the Nytran membrane.) Sizes are indicated in kilodaltons.

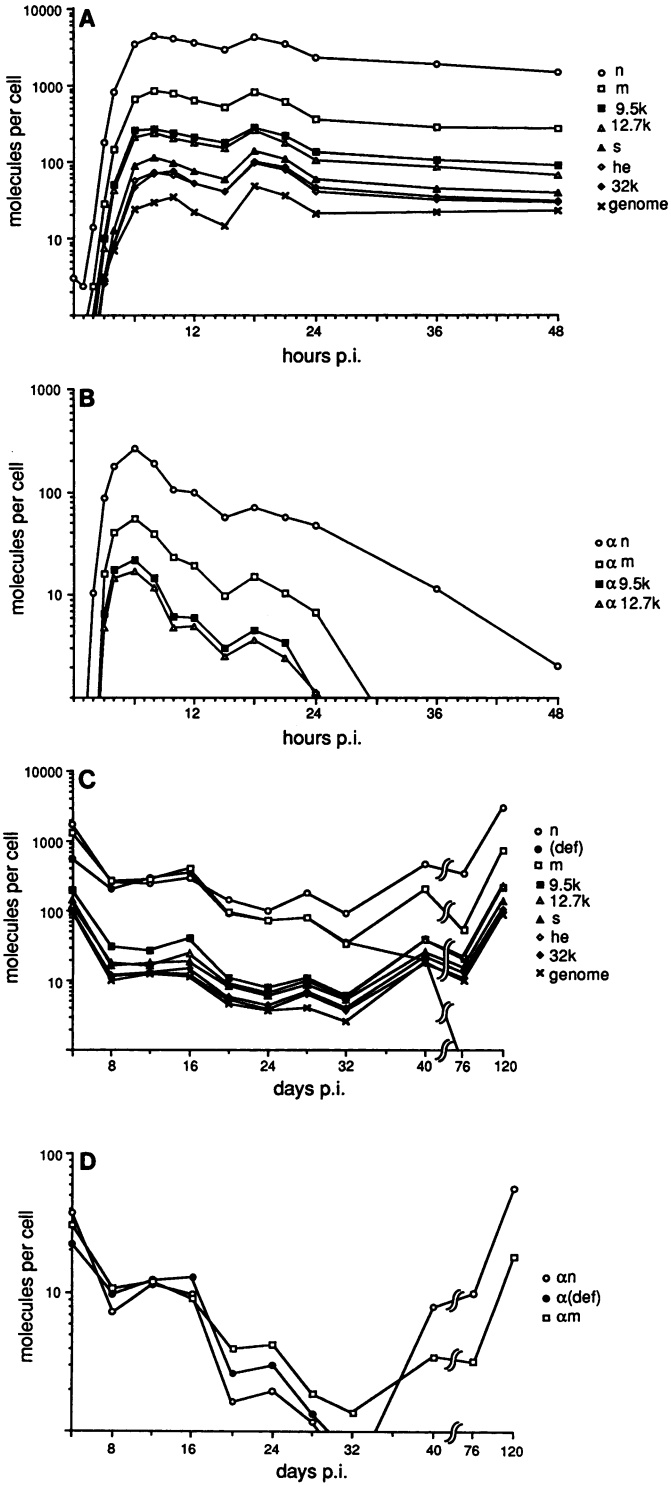

FIG. 3. Kinetics of plus- and minus-strand RNA synthesis. Radiolabeled bands from the corresponding panels in Fig. 2A, B, C, and D were quantitated with the Ambis Radioanalytic Imaging System, and numbers of RNA molecules were determined as described in Materials and Methods.

to decline steadily by approximately 10-fold between 4 and 28 days p.i. and many minus-strand species became undetectable altogether, both plus and minus strands did continue to be made. This conclusion is based first on the fact that infected cells have a doubling time of 2 days, and if plus and minus strands were merely being diluted by cell growth, a half-life of no longer than 2 days would be expected for any given RNA species. Over the first 28 days the half-lives of decay measured approximately 16 days for plus strands and 8 days for minus strands, both considerably longer than 2 days. Second, for αn and αm, and αdef, there was a burst of synthesis at 4 days p.i., the time of the first passage p.i., and for all anti-mRNAs there was a dramatic increase in numbers at 120 days p.i. The increase in synthesis at 4 days p.i. may have been a response to the refeeding of the cells 24 h before harvest. Cells were not refed prior to harvest for any other time point.

We have no explanation for the dramatic increase in the number of anti-mRNAs at 120 days p.i. It may have been that, as in infections with defective interfering viruses, the level of coronavirus genome (polymerase mRNA) had fluctuated inversely with the level of subgenomic molecules sometime prior to the 120-day-p.i. time point. Such a fluctuation might have given rise to a burst of subgenomic RNA synthesis. More experimentation is required to determine whether such a cyclic pattern exists late in persistent coronavirus infection. The decrease in the number of most anti-mRNAs to below detectable limits between 8 h and 120 days p.i. may have been due to the continued replication of virus in only a small fraction of the cells (see below) and the fact that we are determining an average number of molecules per cell.

Two other lines of evidence indicate that the cells remained persistently infected throughout the study. (i) Infectious virus at 10^5 PFU/ml was obtained in the culture supernatant fluids harvested at 40 and 120 days p.i. (ii) Approximately 10% of the cells examined at any time postinfection fluoresced with polyclonal anti-BCV serum (Fig. 4). This compares with approximately 25% of the cells fluorescing during the acute phase of infection (24 hpi).

A defective RNA species appeared by 48 hpi, replicated to abundant numbers, but became undetectable by 76 days p.i. The defective RNA species migrating between n and m first appeared at about 48 hpi (Fig. 2A), and by 12 days p.i. became as abundant as m, the second most abundant mRNA in infected cells. It remained as abundant as m throughout the 32-day period, but was not detectable at 76 and 120 days p.i. We do not yet know the sequence of this species, but it must have been derived in part from the N gene, since it hybridized with N-specific sequence.

DISCUSSION

By demonstrating a 5′ nested set of subgenomic minus-strand RNAs in BCV-infected cells and showing that they have properties of templates for mRNA synthesis, we have, along with our earlier report (22), established that mRNA replication via mRNA replicons is probably a general property of coronaviruses. This property is further supported by a recent report of mRNA-length replicative intermediates in mouse hepatitis virus (MHV)-A59-infected cells (20) and by our finding of mRNA-length minus-strand RNAs in cells infected with MHV-A59 (unpublished). In light of these new data, the transcriptional strategy used by coronaviruses must be reexamined. It can no longer be assumed, for example, that genome-length minus-strand RNA is the only

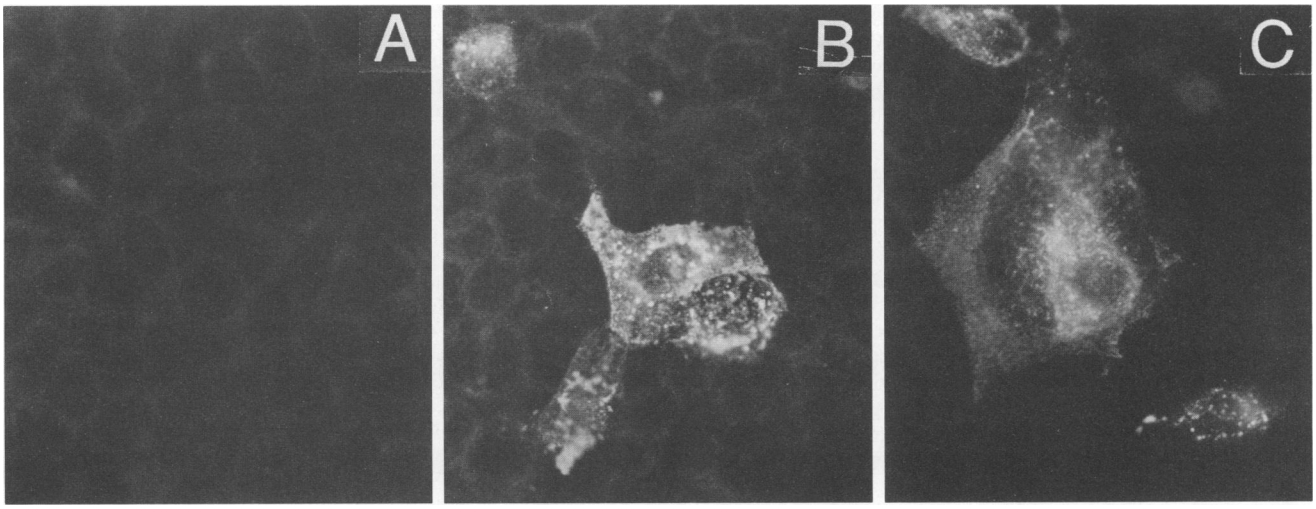

FIG. 4. Immunofluorescence in acutely infected cells at 24 hpi (B) and in persistently infected cells at 120 days p.i. (C). Cells in panel A were uninfected. Cells were stained for cytoplasmic fluorescence as described in Materials and Methods.

template used for mRNA synthesis (7, 11, 13), and it remains to be demonstrated that it in fact can be. Although infectious virion RNA has been demonstrated for avian infectious bronchitis virus (15, 21), MHV (23), and TGEV (3), one-hit kinetics for this activity (demonstrating that a single, full-length genome is sufficient for infectivity) has not been rigorously shown. Until one-hit kinetics for coronavirus genome infectivity or infectivity of the isolated genome is demonstrated, it remains possible that mRNA molecules entering the cell with the virion are the only templates used in their replication (and hence transcription).

Two features of coronavirus mRNA replication observed in our original study with TGEV have been extended by our studies with BCV. The first is that plus-strand mRNAs as well as genome are packaged into virions and can apparently serve as templates for their own replication. For TGEV, genome was packaged most abundantly, showing a 10-fold molar excess over any one of the mRNA species (unpublished). For BCV, however, n and m mRNAs were packaged at least as abundantly as genome (Fig. 2 and unpublished data). In addition to determining the role of packaged mRNAs in their own replication, it will be important to determine what and where the packaging signals are on the molecule. Certainly the signals are specific for plus strands, since no minus strands of any size were detectable in virions (Fig. 2 and data not shown), and their presence on subgenomic mRNAs should facilitate their identification. Since sequences at both the 5′ end (for approximately 80 bases) (12; unpublished data) and 3′ end (for 1,643 bases) (14) are common for all plus-strand species, the packaging signal(s) could theoretically be at either end of the molecule.

The second feature is that whereas the maximal accumulation of minus and plus strands occurred at different times, the initial time and rate of their synthesis appeared to be the same. Additionally, because for BCV the vast majority of cells do not die as a result of acute infection, we were able to observe that minus-strand numbers decreased with a steeper slope than did plus-strand numbers between 7 and 48 hpi (Fig. 3A and B). If we assume that the molecular stabilities of the minus and plus strands are the same, then a more rapid decrease in the population of minus strands late in the acute phase of infection must reflect a decrease in the rate of minus-strand synthesis. Taken together, the concurrent initial synthesis of minus and plus strands and a decrease in the rate of minus-strand synthesis late in the acute phase of infection reflect a pattern described by Sawicki and Sawicki (19) for MHV-A59 RNA synthesis. In their study, no temporal separation between minus- and plus-strand synthesis was found, and plus-strand synthesis continued after minus-strand synthesis had diminished sharply. Our results therefore contrast with those of Brayton et al. (2), who report an early period of minus-strand synthesis followed by a period of plus-strand synthesis.

In general, the kinetics of synthesis of BCV subgenomic RNA in HRT cells paralleled that described for BCV grown in bovine embryo kidney cells (8). One major difference between the two studies, however, is the apparent continued synthesis in the bovine embryo kidney cells (8) of genomic RNA after subgenomic mRNA synthesis had nearly ceased. This may reflect a difference in the cell line used or, more probably, the method of RNA detection. In the study by Keck et al. (8), RNA was metabolically labeled, and thus the longer molecular species would appear to be proportionately more abundant than the same species identified by oligodeoxynucleotide probing.

The continuation of BCV mRNA replication throughout 120 days of persistent infection is consistent with our hypothesis that mRNAs act in a manner similar to defective-interfering (DI) RNAs to attenuate virus replication and thereby establish and maintain virus persistence. Two observations challenge this hypothesis. (i) The abundance of mRNA replicons did not fluctuate inversely with the abundance of genomic replicons (at least throughout the first 40 days p.i., when regular time points were studied) as is the general pattern for DI RNA replication (6). Although common among DI RNAs, this pattern may not be necessary for attenuation by mRNAs. According to our measurements, mRNA numbers are perpetually higher than genome numbers, and the regulating factors that keep genome replication from halting altogether will require quantitation of virus-specific proteins as well as RNAs. (ii) A defective, and possibly interfering, RNA did appear by 48 hpi and continued for at least 40 days. Because its abundance between 2 and 40 days p.i. paralleled that of genome and mRNA replicons, it is difficult to discern how much,

if any, it separately interfered with genome replication and contributed to the establishment of the persistent infection. It is also difficult, without knowing its molecular structure, to hypothesize how the defective species may be competing with genomic replication any more than would mRNA.

Theoretically, sequence arrangements on the defective RNA could have caused a stronger promoter to exist on the 3′ end of both the plus and minus strands (assuming that one of the two possible promoters is stronger), thereby causing the defective RNA to have a replicational advantage (6). If, however, its termini are the same as those of mRNA or genome, it is difficult to see how the defective RNA may be more competitive than an mRNA replicon. Studies to date on the structure of MHV coronavirus DI RNAs show them to have termini that mimic those of the genome (and hence mRNAs) (16, 17). Further study is required to determine the reasons for the instability of the defective species (Fig. 2C and D and 3C and D).

The rapid appearance of the defective RNA (48 h) suggests that it may have been present in small numbers in infecting virions. We predict that this is the case since, as this study shows, coronavirus mRNAs can be readily packaged. For this to have happened, the defective RNA must have been copackaged into the parental virion at the time of plaque purification of virus used for stock inoculum.

Since only some cells in acutely infected or persistently infected monolayers fluoresce, the question arises whether only some cells are infected (i.e., carry the virus genome) or whether all cells are infected and replication is just more attenuated in some than in others. If it can be shown that nonfluorescing cells are infected, then one possible mechanism for attenuation of genome replication in these cells may be that they had received a higher concentration of one or more mRNA species at the time of infection. This might arise as a result of uneven distribution of mRNA species in the infecting virions. Further experimentation is required to determine the infected status of nonfluorescing cells and the distribution of mRNA species among cells in a monolayer.

ACKNOWLEDGMENTS

This work was supported by Public Health Service grant AI14367 from the National Institutes of Health and by U.S. Department of Agriculture grant 82-CRSR-2-1090. M.A.H. was supported by a postdoctoral fellowship from the Swiss National Science Foundation.

LITERATURE CITED

1. **Abraham, S., T. E. Kienzle, W. E. Lapps, and D. A. Brian.** 1990. Deduced sequence of the bovine coronavirus spike protein and identification of the internal proteolytic cleavage site. Virology **176**:296–301.
2. **Brayton, P. R., M. M. C. Lai, C. D. Patton, and S. A. Stohlman.** 1982. Characterization of two RNA polymerase activities induced by mouse hepatitis virus. J. Virol. **42**:847–853.
3. **Brian, D. A., D. E. Dennis, and J. S. Guy.** 1980. Genome of porcine transmissible gastroenteritis virus. J. Virol. **34**:410–415.
4. **Cavanagh, D., D. A. Brian, L. Enjuanes, K. V. Holmes, M. M. C. Lai, H. Laude, S. G. Siddell, W. Spaan, F. Taguchi, and P. J. Talbot.** 1990. Recommendations of the Coronavirus Study Group for the nomenclature of the structural proteins, mRNAs and genes of coronaviruses. Virology **176**:306–307.
5. **Cox, C. J., M. D. Parker, and L. A. Babiuk.** 1989. The sequence of cDNA of bovine coronavirus 32K nonstructural gene. Nucleic Acids Res. **17**:5847.
6. **Holland, J. J.** 1985. Generation and replication of defective viral genomes, p. 77–99. *In* B. N. Fields (ed.), Virology. Raven Press, New York.
7. **Jacobs, L., W. J. M. Spaan, M. C. Horzinek, and B. A. Van Der Zeijst.** 1981. Synthesis of subgenomic mRNAs of mouse hepatitis virus is initiated independently: evidence from UV transcription mapping. J. Virol. **39**:401–406.
8. **Keck, J. G., B. G. Hogue, D. A. Brian, and M. M. C. Lai.** 1988. Temporal regualtion of bovine coronavirus RNA synthesis. Virus Res. **9**:343–356.
9. **Kienzle, T. E., S. Abraham, B. G. Hogue, and D. A. Brian.** 1990. Structure and orientation of expressed bovine coronavirus hemagglutinin-esterase protein. J. Virol. **64**:1834–1838.
10. **King, B., and D. A. Brian.** 1982. Bovine coronavirus structural proteins. J. Virol. **42**:700–707.
11. **Konings, D. A. M., P. J. Bredenbeek, J. F. H. Noten, P. Hogeweg, and W. J. M. Spaan.** 1988. Differential premature termination of transcription as a proposed mechanism for the regulation of coronavirus gene expression. Nucleic Acids Res. **16**:10849–10860.
12. **Lai, M. M. C., R. S. Baric, P. R. Brayton, and S. A. Stohlman.** 1984. Characterization of leader RNA sequences on the virion and mRNAs of mouse hepatitis virus, a cytoplasmic RNA virus. Proc. Natl. Acad. Sci. USA **81**:3626–3630.
13. **Lai, M. M. C., C. D. Patton, and S. A. Stohlman.** 1982. Replication of mouse hepatitis virus: negative-stranded RNA and replicative-form RNA are of genome length. J. Virol. **44**:487–492.
14. **Lapps, W., B. G. Hogue, and D. A. Brian.** 1987. Sequence analysis of the bovine coronavirus nucleocapsid and matrix protein genes. Virology **157**:47–57.
15. **Lomniczi, B.** 1977. Biological properties of avian coronavirus RNA. J. Gen. Virol. **36**:531–533.
16. **Makino, S., and M. M. C. Lai.** 1989. High-frequency leader sequence switching during coronavirus interfering RNA replication. J. Virol. **63**:5285–5292.
17. **Makino, S., C.-K. Shieh, J. G. Keck, and M. M. C. Lai.** 1988. Defective-interfering particles of murine coronavirus: mechanism of synthesis of defective viral RNAs. Virology **163**:104–111.
18. **Parker, M. D., G. J. Cox, D. Deregt, D. R. Fitzpatrick, and L. A. Babiuk.** 1989. Cloning and in vitro expression of the gene for the E3 hemagglutinin glycoprotein of bovine coronavirus. J. Gen. Virol. **70**:155–164.
19. **Sawicki, S. G., and D. L. Sawicki.** 1986. Coronavirus minus-strand RNA synthesis and effect of cycloheximide on coronavirus RNA synthesis. J. Virol. **57**:328–334.
20. **Sawicki, S. G., and D. L. Sawicki.** 1990. Coronavirus transcription: subgenomic mouse hepatitis virus replicative intermediates function in RNA synthesis. J. Virol. **64**:1050–1056.
21. **Schochetman, G., R. H. Stevens, and R. W. Simpson.** 1977. Presence of infectious polyadenylated RNA in the coronavirus avian infectious bronchitis virus. Virology **77**:772–782.
22. **Sethna, P. B., S.-L. Hung, and D. A. Brian.** 1989. Coronavirus subgenomic minus-strand RNAs and the potential for mRNA replicons. Proc. Natl. Acad. Sci. USA **86**:5626–5630.
23. **Wege, H., A. Muller, and V. ter Meulen.** 1978. Genomic RNA of the murine coronavirus JHM. J. Gen. Virol. **41**:217–227.